

RSC Advances



This is an *Accepted Manuscript*, which has been through the Royal Society of Chemistry peer review process and has been accepted for publication.

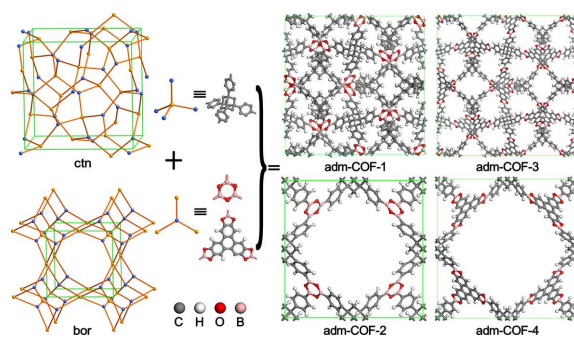
Accepted Manuscripts are published online shortly after acceptance, before technical editing, formatting and proof reading. Using this free service, authors can make their results available to the community, in citable form, before we publish the edited article. This *Accepted Manuscript* will be replaced by the edited, formatted and paginated article as soon as this is available.

You can find more information about *Accepted Manuscripts* in the [Information for Authors](#).

Please note that technical editing may introduce minor changes to the text and/or graphics, which may alter content. The journal's standard [Terms & Conditions](#) and the [Ethical guidelines](#) still apply. In no event shall the Royal Society of Chemistry be held responsible for any errors or omissions in this *Accepted Manuscript* or any consequences arising from the use of any information it contains.

Table of contents

Four 1,3,5,7-tetraphenyladamantane based covalent-organic frameworks (adm-COFs) have been designed under ctn or bor net topology as hydrogen storage materials.



Design of 3D 1,3,5,7-tetraphenyladamantane based covalent-organic frameworks as hydrogen storage materials

Xiao-Dong Li,^{*1} Jing-Hua Guo,² Hong Zhang,³ Xin-Lu Cheng,⁴ Xiu-Ying Liu¹

¹*College of Science, Henan University of Technology, Zhengzhou 450001, China*

²*School of Physics Science, University of Jinan, Jinan 250022, China*

³*College of Physical Science and Technology, Sichuan University, Chengdu 610065, China*

⁴*The Institute of Atomic and Molecular Physics, Sichuan University, Chengdu 610065, China*

Abstract

A new type of 1,3,5,7-tetraphenyladamantane based covalent-organic frameworks (adm-COFs) was designed under the ctn and bor net topology with the method of molecular mechanics. The computed results reveal that all four designed adm-COFs exhibit extremely high porosity (86% - 95%) and large H₂ accessible surface area (5967 - 6709 m²/g). The grand canonical Monte Carlo (GCMC) method was employed to simulate the adsorption isotherms of H₂ gas in these adm-COFs at 77 K and 298 K. The simulated results reflect that at 77 K and 100 bar adm-COF-4 has the highest gravimetric H₂ adsorption capacity of 38.36 wt%, while adm-COF-1 owns the highest volumetric H₂ adsorption capacity of 60.71 g/L. Impressively, the gravimetric H₂ adsorption capacity of adm-COF-1 can reach up to 5.81 wt% under 100 bar at room temperature, which is very close to criterion of 6 wt% for the practical application of hydrogen at room temperature set by U.S. Department of Energy. In addition, the possible schemes for synthesizing these adm-COFs have been proposed.

* Corresponding author: Xiao-Dong Li, E-mail: dragoninstream@gmail.com

Keywords: adm-COF, 1,3,5,7-tetraphenyladamantane, hydrogen adsorption, grand canonical Monte Carlo

Introduction

It is well-known that the fossil fuels on our planet are being used up and hence new energy carriers must be found and exploited. For the purpose of environmental protection, the new energy carriers must be clean and pollution-free. Hydrogen has been for long recognized as an unexceptionable candidate because of its advantages in comparison with other possible fuels.^{1,2} However, the safe and efficient storage is one of the significant challenges for the wide use of hydrogen as energy carriers due to the serious drawbacks of traditional hydrogen storage methods,^{1,3} i.e. high-pressure gas or cryogenic liquefaction. Currently, more and more attentions have been paid to the material-based hydrogen storage methods both in experimental and theoretical fields.⁴⁻⁷ Consequently, plenty of materials including hydrides,^{8,9} porous frameworks,¹⁰⁻¹³ hydrogen clathrates,^{14, 15} and so on,^{16, 17} have been proposed as hydrogen storage media. The U.S. Department of Energy (DOE) has set some short-time goals for commercialized on-board hydrogen storage systems.¹⁸ The goal for 2017 requires the hydrogen gravimetric density of 4.5 wt% and volumetric capacity of 40 g/L at near ambient temperature and applicable pressure (less than 100 bar). Unfortunately, none of the existing materials can meet all requirements established by the U.S. DOE. Thus, to search for new materials or modify the existing materials with improved hydrogen storage properties is still an urgent issue in the field of hydrogen storage.

Covalent-organic frameworks (COFs) are one type of emerging porous crystalline

architecture with two-dimension (2D) or three-dimension (3D) structures constructed by strong covalent bonds between the light elements such as C, H, O, B, N and Si.¹⁹⁻²² COFs have large pore volumes, high surface areas, and very low density,¹⁹ all of which are advantageous to the gas storage. Therefore, many investigations have been performed to study the hydrogen storage properties of COFs or their modified counterparts.^{2, 12, 23-26} At the same time, many novel COFs have been reported either by experimental synthesis or by theoretical design.^{2, 27-29} For example, Furukawa and Yaghi measured the H₂, CH₄, and CO₂ adsorption isotherms on a series of COFs at 1-85 bar and 77 -298 K in experiment.²³ They well described the gas uptake behavior and capacity of these COFs by classifying them into three groups based on their structural dimensions and corresponding pore sizes. Mendoza-Cortes et al, calculated the H₂ uptake at 298 K for several Li-, Na-, and K-metalized COFs by combining quantum mechanics calculations and grand canonical Monte Carlo (GCMC) simulations.²⁴ Compared with their pristine counterparts, these metalized COFs possess enhanced hydrogen storage capacity at the studied condition. Additionally, Klontzas et al. studied hydrogen storage properties of four theoretically designed 3D COFs.²⁷ Better yet, gravimetric uptake of one of these new COFs can overpass the value of 25 wt % at 77 K and reach the U.S. DOE's target of 6 wt % at room temperature. Using the similar methods, Mendoza-Cortes designed fourteen new COFs that can adsorb large amounts of methane up to 300 bar at 298 K.²⁸ Also, by inserting the pyridine molecules into the 2D COF-1 layers, Kim et al. proposed several pillared COFs (PCOFs) to expose buried framework surfaces to pores.²⁹ With this approach, the PCOFs have significantly improved gravimetric and volumetric hydrogen storage capacities of 8.8-10.0 wt% and 58.7-61.7 g L⁻¹, respectively.

Insert Figure 1

Probing into the net topologies of 3D COFs,¹⁹ we find that the 3D COFs are mainly constructed through ctn or bor topology³⁰ with tetrahedron and triangle building units. Typically, COF-102, COF-103, COF-105 have ctn topology while COF-108 possesses bor topology, and furthermore COF-105 and COF-108 contain the same build units but different topology structures. Also, the theoretically designed 3D COFs are also conformed to these two net topologies with various build units.^{27, 28} Motivated and inspired by these studies, we designed four novel 3D porous covalent frameworks based on two planar triangular units appeared widely in 3D COFs¹⁹ and one tetrahedral building unit (1,3,5,7-tetraphenyladamantane) shown in Fig. 1. 1,3,5,7-tetraphenyladamantane is a rigid tetrahedral building block with similar geometry characteristics^{31, 32} with tetraphenylmethane which appears frequently in the structures of 3D COFs in experiments.^{19, 22} In a previous study,³² Schilling et al. synthesized a series of rigid tetrahedral organic building units from tetraphenylmethane and 1,3,5,7-tetraphenyladamantane precursors through Suzuki–Miyaura and Sonogashira cross-coupling reactions. Furthermore, adamantane based tetrahedral units have been widely used for synthesizing various nanostructures.³³⁻³⁶ In one of our previous work, we also designed three types of adamantane based aromatic frameworks with extremely high hydrogen storage capacity.³⁷ However, to the best of our knowledge, there is no report on 1,3,5,7-tetraphenyladamantane based crystalline porous COFs. Hence, in present work, we designed four types of 1,3,5,7-tetraphenyladamantane based COFs with ctn or bor net

structures and investigated their hydrogen storage properties.

Design and calculation methods

The *ctn* ($I\bar{4}3m$ space group) and *bor* ($P\bar{4}3m$ space group) net topologies have been considered to be the most stable structures for the 3, 4 frameworks.^{19, 30, 38} As shown Fig. 1, the *ctn* and *bor* net structures are both comprised of the tetrahedral and triangular units. Conceptually, by replacing the tetrahedral and triangular sites in *ctn* and *bor* net with suitable building units, two types of framework materials can be obtained. Herein, we build four types of adm-COFs termed as adm-COF-1, adm-COF-2, adm-COF-3 and adm-COF-4 based on 1,3,5,7-tetraphenyladamantane and the two planer triangular units, as depicted in Fig. 1. To construct the adm-COFs, we first build the geometric structures of the tetrahedral ligand (1,3,5,7-tetraphenyladamantane) and the two triangular ligands (B_3O_3 and $C_{18}H_6O_6B_3$). Then we add the irreducible representation of the ligands into the corresponding space group of the topological structure. None of the ligands produces the lower symmetrical structure. Here the adm-COF-1 and adm-COF-3 follow $I\bar{4}3m$ space group symmetry, while adm-COF-2 and adm-COF-4 obey the $P\bar{4}3m$ space group symmetry. In addition, the adm-COF-1 and adm-COF-2 (also the adm-COF-3 and adm-COF-4) are built with the same chemical building blocks, as can be seen clearly in the Fig. 1.

Insert Table 1

After the construction of adm-COFs, we optimized the adm-COFs using the Forcite Plus

module in Material Studio. The Dreiding force field³⁹ and the “Ultra-fine” criterion are used for structural optimization. During the optimization, no space group symmetry constraints were imposed on the frameworks and all the bond lengths, angles, and cell parameters were optimized to get the best framework structures. The geometries are optimized until the remaining atomic forces are less than 0.0001 kcal/(mol·Å) on each atom and the energy convergence criterion is chosen as 1.0×10^{-5} kcal/mol between two steps. Based on the optimized structures, the GCMC simulations were performed to obtain the hydrogen adsorption isotherms for four porous frameworks. During the simulations, the Van der Waals interactions between the H₂ molecule and the frameworks are treated as 12-6 Lennard-Jones (LJ) potential as shown in equation (1). The potential parameters of the framework atoms were taken from the Dreiding force field of Mayo et al,³⁹ and the potential parameters of H₂ molecules were from the work of Buch,⁴⁰ where a united-atom model for H₂ molecule is employed. All the potential parameters used in the present work are presented in Table 1. The cross-interaction parameters between different types of atoms are calculated using the Lorentz–Berthelot mixing rules shown in equation (2) and (3). In addition, the LJ interactions were calculated with a spherical cut-off value of 13 Å.

$$U_{LJ} = -4\epsilon_{ij} \left[\left(\frac{\sigma_{ij}}{r_{ij}} \right)^6 - \left(\frac{\sigma_{ij}}{r_{ij}} \right)^{12} \right] \quad (1)$$

$$\sigma_{ij} = (\sigma_{ii} + \sigma_{jj}) / 2 \quad (2)$$

$$\epsilon_{ij} = \sqrt{\epsilon_{ii} \epsilon_{jj}} \quad (3)$$

The adsorption of H₂ gas were calculated using Monte Carlo (MC) simulations in the grand canonical ensemble (μ VT) with the code Music⁴¹, where the chemical potential, temperature, and volume are constant. Chemical potentials were converted to fugacity with

the Peng-Robinson equation of state.⁴² During the simulations, the 2×2×2 supercells for all frameworks were adopted and the periodic condition was employed in all three dimensions. The frameworks were frozen during the simulations. The number of total Monte Carlo steps in a typical GCMC simulation was 2×10⁷. The first half steps were used for equilibration and the second half steps were used for ensemble average. One Monte Carlo step was consisted of three trivial moves of H₂ molecules, namely, insertion of a new molecule, deletion of an existing molecule, or translation of an existing molecule. The veracity of the employed force field parameters and the simulation method were validated in our previous paper.³⁷ In addition, the excess H₂ adsorption amounts (N_{exc}) were calculated by equation (4)

$$N_{exc} = N_{abs} - \rho V_p \quad (4)$$

Here, N_{abs} is the absolute H₂ adsorption amounts, ρ is the density of the H₂ gas under the thermodynamics conditions studied and V_p is the pore volume of the adsorbent. The density of H₂ gas under a given pressure and temperature was computed by Peng-Robinson equation of state.⁴² Finally, the H₂ adsorption amounts were converted to gravimetric or volumetric H₂ adsorption capacities to obtain H₂ adsorption isotherms under certain temperature. The pore volume of these porous materials were evaluated with the method proposed by Talu and Myers.⁴³ They suggested that the pore volume of porous material could be estimated by the amounts of adsorbed helium molecules (N_a) at low pressure (P) and room temperature (T_0) with equation (5)

$$V_p = N_a K_B T_0 / P \quad (5)$$

where K_B refers to the Boltzmann constant.

Additionally, the isosteric heat of adsorption of H₂ molecule (Q_{st}) was calculated with the

equation (6)⁴⁴

$$Q_{st} = RT - \left(\frac{\partial \langle v \rangle}{\partial \langle N \rangle} \right)_T \quad (6)$$

Here, R denotes the ideal gas constant, T is the temperature, v is potential energy of the adsorbed phase, N is the number of molecules in the adsorbed phase, and the angular bracket indicates an ensemble average.

Results and discussions

Based on the structural optimization, we get the final geometry structures of these porous frameworks. To know whether the frameworks still maintain the space group symmetry, we search for their symmetries in the final 3D models using the specified tolerance of 10^{-5} Å with Materials Studio Visualizer.⁴⁵ The results reveal that all four adm-COFs keep the same space group symmetries as the original designed ones under the tolerance of 10^{-5} Å. The structural and physical parameters of four adm-COFs are listed in Table 2. The space group symmetries and coordinates of these frameworks are provided in the supporting information. As can be seen in Table 2, although they are consisted of the same building blocks, adm-COF-1 (also adm-COF-3) has the larger unit cell length than that of adm-COF-2 (adm-COF-4) duo to their different topological structures. On the other hand, under the same space group symmetry, adm-COF-3 (also adm-COF-4) has much larger unit cell length than that of adm-COF-1 (adm-COF-2) attributed to the fact that adm-COF-3 and adm-COF-4 possess much larger triangular building units than that of adm-COF-1 and adm-COF-2. In addition, the densities of four adm-COFs are all very low (0.14-0.30 g/cm³), especially for adm-COF-3 and adm-COF-4, which indicates the high porosity of these materials. To our knowledge, the

porous materials with the lowest density are reported for COF-108 (0.17 g/cm³) and COF-105 (0.18 g/cm³)^{19, 46} in experiment. Impressively, adm-COF-3 and adm-COF-4 own even lower density than COF-105 and COF-108, which reflects that they have entered the lists of porous materials with the lowest density.

Insert Table 2

The pore size is an important index to judge the performance of porous materials. Based on the amounts of Helium molecules adsorbed in these adm-COFs at the pressure of 0.1-1 bar and the temperature of 298 K, their pore volumes were calculated by equation (5) and the results are presented in Table 2. It can be found that the pore volume of four adm-COFs confirmed the sequence adm-COF-1 < adm-COF-2 < adm-COF-3 < adm-COF-4, which is just opposite to the sequence of density. To gain a concrete image of porosity, the percent pore volumes of four adm-COFs are evaluated and they are 86.18 %, 87.39 %, 94.17 %, and 94.51 % for adm-COF-1 to adm-COF-4, respectively. Excitingly, the very high porosity of all four adm-COFs is comparable with COF-105 (88.22%), COF-108 (88.84%) and PAF-1 (77.60%),^{19, 46, 47} which are all high-porosity materials with excellent hydrogen storage properties. Besides the pore volume, the surface area is also a key factor for the gas adsorption in the porous materials. Herein, we estimate the surface area of these adm-COFs using the accessible surface areas. The accessible surface areas of the adm-COFs were computed by a numerical Monte Carlo integration technique proposed by Frost et al.⁴⁸ It was performed by “rolling” a probe H₂ molecule with a diameter equal to the LJ σ parameter of H₂

molecule (2.958 Å). The probe was randomly inserted around the surface of each framework atom with a diameter equal to their LJ σ parameters one by one to test for overlap. The fraction of probes that did not overlap with other framework atoms was used to calculate the accessible surface area. Surface area estimated using this method is highly dependent on the probe size used for measurement, and calculating the surface area using a H₂ probe molecule provides the amount of area accessible to H₂ molecules. As shown in Table 2, the H₂ accessible surface areas for four adm-COFs confirm the sequence adm-COF-2 < adm-COF-1 < adm-COF-4 < adm-COF-3. Ascribed to the larger triangular building unit, adm-COF-3 and adm-COF-4 have the larger surface areas than adm-COF-1 and adm-COF-2. Additionally, since ctn topology net possesses more complicated net structures than bor topology net, adm-COF-1 (adm-COF-3) has larger surface area than adm-COF-2 (adm-COF-4). Anyhow, all adm-COFs reported here are on a par with the porous materials with the highest surface area. To our knowledge, the highest surface area reported for MOF materials is claimed for MOF-210, which has a Brunauer–Emmett–Teller (BET) surface area of 6240 m²/g and a Langmuir surface area of 10400 m²/g.⁴⁹ In addition, highest surface area reported for COF materials is 4210 m²/g (BET) in COF-103 up to now.¹⁹ Also, PAF-1 owns a very high BET surface area of 5600 m²/g and a Langmuir surface area of 7100 m²/g.⁴⁷ The H₂ accessible surface areas of these adm-COFs (5968-6696 m²/g) listed in Table 2 testify that they are all porous materials with large surface area. The high porosity and larger H₂ accessible surface area of these designed adm-COFs forebodes good hydrogen storage properties of these porous materials.

Insert Figure 2

The adsorption isotherms of H₂ in four adm-COFs from 0.1 bar to 100 bar at 77 K are shown in Fig. 2. As depicted in Fig. 2, both absolute gravimetric and volumetric H₂ adsorption capacities of four adm-COFs increase gradually with the rise of H₂ pressure, while the excess H₂ adsorption capacities reach their maximums at low H₂ pressure. It can be seen in Fig. 2(a) that the absolute gravimetric H₂ adsorption capacity of adm-COF-1 is higher than that of adm-COF-2 at $P < 30$ bar, whereas it is reversed at $P \geq 30$ bar. While for adm-COF-3 and adm-COF-4, the absolute gravimetric H₂ adsorption capacity of adm-COF-4 is higher than that of adm-COF-3 at all the pressure studied. The maximum absolute gravimetric H₂ adsorption capacities are 20.66 wt%, 22.08 wt%, 32.87 wt% and 38.36 wt% for adm-COF-1, adm-COF-2, adm-COF-3 and adm-COF-4, respectively. At the same time, the maximum excess gravimetric H₂ adsorption capacities are 10.60 wt% for adm-COF-1 at 30 bar, 12.80 wt% for adm-COF-2 at 40 bar, 12.08 wt% for adm-COF-3 at 70 bar and 15.13 wt% for adm-COF-4 at 70 bar. On the other hand, as depicted in Fig. 2 (b), the absolute volumetric H₂ adsorption capacities for four adm-COFs obey the sequence of adm-COF-1 > adm-COF-2 > adm-COF-4 > adm-COF-3, which is basically contrary to that of the absolute gravimetric H₂ adsorption capacities. The maximum absolute (excess) volumetric H₂ adsorption capacities are 60.71 g/L (36.93 g/L at 30 bar), 59.06 g/L (34.12 g/L at 40 bar), 49.18 g/L (17.88 g/L at 70 bar) and 51.70 g/L (20.21 g/L at 70 bar) for adm-COF-1 to adm-COF-4, respectively. All these results reveal that the adm-COFs have excellent hydrogen storage capacities at 77 K.

Insert Figure 3

Since the practical application of hydrogen should be at room temperature, we also calculated their hydrogen uptake at 298 K. As can be seen in Fig. 3, both gravimetric and volumetric H₂ adsorption capacities increase linearly with the rise of H₂ pressure at 298 K. This is the character of Henry's linear isotherm equation.^{50, 51} The Henry's linear isotherm equation is $n = KP$, where n is the adsorbed amount per unit weight of adsorbent (wt %), P is the adsorbate gas pressure at equilibrium (bar), and K is the Henry's law constant (wt % per bar). The fitted linear isotherm equations for four adm-COFs and their degrees of linear correlation are listed in Fig. 3 (a). The subscripts 1 to 4 in these equations denote the corresponding equations and degrees of linear correlation are for adm-COF-1 to adm-COF-4. The excellent linearity reveals that the H₂ adsorption capacity in these adm-COFs is proportional to the pore volume and virtually independent of binding energy or surface area at the room temperature. As shown in Fig. 3, the gravimetric H₂ adsorption capacities follow the sequence of adm-COF-1 < adm-COF-2 < adm-COF-3 < adm-COF-4 at all pressure studied, which is indeed the same sequence as the size of the pore volume deduced from Table 2. In Fig. 3, the maximum absolute gravimetric (volumetric) H₂ adsorption capacities are 2.73 wt% (8.03 g/L), 2.98 wt% (7.98 g/L), 4.65 wt% (6.96 g/L) and 5.81 wt% (7.83 g/L) for adm-COF-1 to adm-COF-4 at 100 bar, respectively. Surprisingly, the maximum gravimetric H₂ adsorption capacities for adm-COF-3 and adm-COF-4 has exceeded U.S. DOE's goal (4.5 wt%) for 2017.¹⁸ Especially, the adm-COF-4 possess a maximum gravimetric H₂ adsorption capacity of 5.81 wt%, which does very approach the capacity (6 wt%) for practical

application of hydrogen at room temperature proposed by U.S. DOE. However, it is a pity that four adm-COFs all have low volumetric H₂ adsorption capacity at room temperature, which again indicates the dependence of H₂ adsorption capacity on the pore volume. To enhance the volumetric H₂ adsorption capacity of these adm-COFs, some modified methods must be adopted, which is being carried out in the subsequent studies.

Insert Figure 4

We have computed the isosteric heats of adsorption of H₂ molecule in four adm-COFs at both 77 K and 298 K by equation (6). Table 2 lists the average isosteric heat of adsorption of H₂ molecule in each adm-COF at 77 K and 298 K. It can be found that adm-COF-1 and adm-COF-2 have the larger average isosteric heat of adsorption of H₂ than adm-COF-3 and adm-COF-4. This can be attributed to the smaller triangular units of adm-COF-1 and adm-COF-2, which introduces the smaller cavities than adm-COF-3 and adm-COF-4 and hence produces the stronger the Van der Waals interactions between the H₂ molecules and the frameworks. On the other hand, due to the different net topologies of four adm-COFs, adm-COF-2 (adm-COF-4) with bor topology can adsorb H₂ molecules with larger average isosteric heat of adsorption than adm-COF-1 (adm-COF-3) with bor topology. In addition, it needs to point that isosteric heats of adsorption for H₂ molecule in four adm-COFs are all very small. Some previous work have pointed that the value of isosteric heat larger than 15 kJ/mol is likely to be needed for practical hydrogen storage.⁷ To improve the isosteric heats of adsorption of H₂ molecule in adm-COFs, some modified methods can be adopted.

This problem is consistent with the low volumetric H₂ adsorption capacity at room temperature, which has discussed in the previous paragraph.

Furthermore, to understand the adsorption behaviors of H₂ gas in the frameworks at a molecular level, we examined the snapshots of four adm-COF structures with the adsorbed H₂ molecules at both 77 K and 298 K. Here, we typically show the snapshots of four adm-COFs with adsorbed H₂ molecules at 77 K and 100 bar in Fig. 4. From these snapshots, we find that the triangular units, especially the B₃O₃ and BC₂O₂ rings, are the preferential adsorption sites for H₂ molecules. During the adsorption process, the H₂ molecules are first adsorbed on the triangular units at low H₂ pressure. With the increase of the H₂ pressure, the H₂ molecules begin to occupy the corner sites near the tetrahedral units. At last, the H₂ molecules accommodate the cavities far from the framework surface for further rise of H₂ pressure.

Finally, we proposed two possible schemes to synthesize these adm-COFs. We chose tetra(4-dihydroxyborylphenyl)adamantane (TBPA) as tetrahedral building unit (Fig. 5A) and the hexahydroxytriphenylene (HHTP) as triangular building block (Fig. 5B). In principle, an infinite number of possible nets may result from linking tetrahedrons with triangles. However, analysis of previous assembly reactions suggests that the most symmetric nets are the most likely to result in an unbiased system and that those with just one kind of link will be preferred and are thus the best to target.¹⁹ In the present case of linking tetrahedral and triangular building blocks, the only known nets meeting the above criteria are the net with *ctn* and *bor*^{19, 30} topologies shown in Fig. 1. Based on these backgrounds, we proposed the synthesis schemes (R1 and R2) for these adm-COFs, as depicted in Fig. 5. As shown in Fig. 5,

adm-COF-1 and adm-COF-2 may be synthesized by self-condensation of TBPA to form B_3O_3 rings (Fig. 5C), while adm-COF-3 or adm-COF-4 can be obtained by co-condensation of TBPA and HHTP to form C_2O_2B rings (Fig. 5D). To form the 3D ctn and bor structures, the use of rigid, planar triangular units, such as B_3O_3 rings, requires that rotational freedom exist at the tetrahedral nodes.

Conclusions

In conclusion, four novel 3D 1,3,5,7-tetraphenyladamantane based COFs were designed and proposed as hydrogen storage materials. The pore volume, porosity and H_2 accessible surface area were estimated based on the optimized adm-COF structures. The computed results reveal that all four adm-COFs belong to the porous materials with high porosity and large surface area. The GCMC simulations reveal that adm-COF-4 possesses the highest gravimetric H_2 adsorption capacity while adm-COF-1 has the highest volumetric H_2 adsorption capacity among four adm-COFs at both 77 K and 298 K. Surprisingly, the maximum gravimetric H_2 adsorption capacity for adm-COF-4 has exceeded U.S. DOE's goal (4.5 wt%) for 2017 and also very approaches the capacity (6 wt%) for practical use of hydrogen at room temperature. In addition, the possible schemes for synthesizing these adm-COFs have been proposed. Although to synthesize the tailored adm-COFs proposed here still require further efforts in future, we hope that knowledge gained from this study will motivate some inspirations for developing the corresponding experiments.

Supporting information

The space group symmetries and coordinates of these adm-COF materials are provided in the supporting information.

Acknowledgements

This work was supported by the Talent Introduction Foundation of Henan University of Technology (No. 2013BS039) and the National Natural Science Foundation of China (Grant No. 11304079).

References

1. L. Schlapbach and A. Züttel, *Nature*, 2001, **414**, 353-358.
2. E. Tylianakis, E. Klontzas and G. E. Froudakis, *Nanoscale*, 2011, **3**, 856-869.
3. U. Eberle, M. Felderhoff and F. Schuth, *Angew. Chem. Int. Ed.*, 2009, **48**, 6608-6630.
4. H. Reardon, J. M. Hanlon, R. W. Hughes, A. Godula-Jopek, T. K. Mandal and D. H. Gregory, *Energy Environ. Sci.*, 2012, **5**, 5951-5979.
5. S.-H. Jhi and J. Ihm, *MRS Bull.*, 2011, **36**, 198-204.
6. P. Jena, *J. Phys. Chem. Lett.*, 2011, **2**, 206-211.
7. A. W. C. van den Berg and C. O. Arean, *Chem. Commun.*, 2008, 668-681.
8. S. Orimo, Y. Nakamori, J. R. Eliseo, A. Züttel and C. M. Jensen, *Chem. Rev.*, 2007, **107**, 4111-4132.
9. B. Sakintuna, F. Lamari-Darkrim and M. Hirscher, *Int. J. Hydrogen Energy*, 2007, **32**, 1121-1140.
10. V. C. Menon and S. Komarneni, *J. Porous Mater.*, 1998, **5**, 43-58.
11. S. Ma and H. C. Zhou, *Chem. Commun.*, 2010, **46**, 44-53.
12. B. Assfour and G. Seifert, *Microporous Mesoporous Mater.*, 2010, **133**, 59-65.
13. E.-Y. Chen, Y.-C. Liu, M. Zhou, L. Zhang and Q. Wang, *Chem. Eng. Sci.*, 2012, **71**, 178-184.
14. P. K. Chattaraj, S. Bandaru and S. Mondal, *J. Phys. Chem. A*, 2011, **115**, 187-193.
15. V. V. Struzhkin, B. Miltzer, W. L. Mao, H.-k. Mao and R. J. Hemley, *Chem. Rev.*, 2007, **107**, 4133-4151.
16. Y. Zhao, Y.-H. Kim, A. C. Dillon, M. J. Heben and S. B. Zhang, *Phys. Rev. Lett.*, 2005, **94**, 155504.
17. J. Carrete, R. C. Longo, L. J. Gallego, A. Vega and L. C. Balbás, *Phys. Rev. B*, 2012, **85**, 125435.
18. <http://www1.eere.energy.gov/hydrogenandfuelcells/mypp/>.
19. H. M. El-Kaderi, J. R. Hunt, J. L. Mendoza-Cortes, A. P. Cote, R. E. Taylor, M. O'Keeffe and O. M. Yaghi, *Science*, 2007, **316**, 268-272.
20. A. P. Cote, A. I. Benin, N. W. Ockwig, M. O'Keeffe, A. J. Matzger and O. M. Yaghi, *Science*, 2005, **310**, 1166-1170.
21. E. L. Spitler, J. W. Colson, F. J. Uribe-Romo, A. R. Woll, M. R. Giovino, A. Saldivar and W. R. Dichtel, *Angew. Chem. Int. Ed.*, 2012, **51**, 2623-2627.

22. F. J. Uribe-Romo, J. R. Hunt, H. Furukawa, C. Klock, M. O'Keeffe and O. M. Yaghi, *J. Am. Chem. Soc.*, 2009, **131**, 4570-4571.
23. H. Furukawa and O. M. Yaghi, *J. Am. Chem. Soc.*, 2009, **131**, 8875-8883.
24. J. L. Mendoza-Cortes, S. S. Han and W. A. Goddard, *J. Phys. Chem. A*, 2012, **116**, 1621-1631.
25. J. L. Mendoza-Cortes, S. S. Han, H. Furukawa, O. M. Yaghi and W. A. Goddard, 3rd, *J. Phys. Chem. A*, 2010, **114**, 10824-10833.
26. M. Dogru, A. Sonnauer, A. Gavryushin, P. Knochel and T. Bein, *Chem. Commun.*, 2011, **47**, 1707-1709.
27. E. Klontzas, E. Tylanakis and G. E. Froudakis, *Nano Lett.*, 2010, **10**, 452-454.
28. J. L. Mendoza-Cortes, T. A. Pascal and W. A. Goddard, *J. Phys. Chem. A*, 2011, **115**, 13852-13857.
29. D. Kim, D. H. Jung, K. H. Kim, H. Guk, S. S. Han, K. Choi and S. H. Choi, *J. Phys. Chem. C*, 2012, **116**, 1479-1484.
30. O. Delgado-Friedrichs, M. O'Keeffe and O. M. Yaghi, *Acta Crystallogr. Sect. A*, 2006, **62**, 350-355.
31. O. Plietzsch, C. I. Schilling, M. Nieger, T. Muller and S. Bräse, *Tetrahedron: Asymmetry*, 2010, **21**, 1474-1479.
32. C. I. Schilling, O. Plietzsch, M. Nieger, T. Muller and S. Bräse, *Eur. J. Org. Chem.*, 2011, **2011**, 1743-1754.
33. H. Lim and J. Y. Chang, *Macromolecules*, 2010, **43**, 6943-6945.
34. A. Lemmerer, J. Bernstein and M. A. Spackman, *Chem. Commun.*, 2012, **48**, 1883-1885.
35. R. Coratger, B. Calmettes, Y. Benjalal, X. Bouju and C. Coudret, *Surf. Sci.*, 2012, **606**, 444-449.
36. G. A. Senchyk, A. B. Lysenko, D. Y. Naumov, V. P. Fedin, H. Krautscheid and K. V. Domasevitch, *Inorg. Chem. Commun.*, 2010, **13**, 1576-1579.
37. X. D. Li, H. Zhang, Y. J. Tang and X. L. Cheng, *Phys. Chem. Chem. Phys.*, 2012, **14**, 2391-2398.
38. R. Schmid and M. Tafipolsky, *J. Am. Chem. Soc.*, 2008, **130**, 12600-12601.
39. S. L. Mayo, B. D. Olafson and W. A. Goddard, *J. Phys. Chem.*, 1990, **94**, 8897-8909.
40. V. Buch, *J. Chem. Phys.*, 1994, **100**, 7610-7629.
41. A. Gupta, S. Chempath, M. J. Sanborn, L. A. Clark and R. Q. Snurr, *Mol. Simul.*, 2003, **29**, 29-46.
42. D. Y. Peng and D. B. Robinson, *Ind. Eng. Chem. Fundam.*, 1976, **15**, 59-64.
43. O. Talu and A. L. Myers, *AIChE J.*, 2001, **47**, 1160-1168.
44. R. Q. Snurr, A. T. Bell and D. N. Theodorou, *J. Phys. Chem.*, 1993, **97**, 13742-13752.
45. M. Studio, Accelrys Inc, San Diego, CA.
46. D. Cao, J. Lan, W. Wang and B. Smit, *Angew. Chem. Int. Ed.*, 2009, **48**, 4730-4733.
47. T. Ben, H. Ren, S. Ma, D. Cao, J. Lan, X. Jing, W. Wang, J. Xu, F. Deng, J. M. Simmons, S. Qiu and G. Zhu, *Angew. Chem. Int. Ed.*, 2009, **48**, 9457-9460.
48. H. Frost, T. Duren and R. Q. Snurr, *J. Phys. Chem. B*, 2006, **110**, 9565-9570.
49. H. Furukawa, N. Ko, Y. B. Go, N. Aratani, S. B. Choi, E. Choi, A. O. Yazaydin, R. Q. Snurr, M. O'Keeffe, J. Kim and O. M. Yaghi, *Science*, 2010, **329**, 424-428.
50. J. Palgunadi, H. S. Kim, J. M. Lee and S. Jung, *Chem. Eng. Process.*, 2010, **49**, 192-198.
51. L. Zhou and Y. P. Zhou, *Ind. Eng. Chem. Res.*, 1996, **35**, 4166-4168.

Figure captions

Table 1 The LJ potential parameters of H₂, He molecules and all the framework atoms used in the present work.

Table 2 Unit cell parameters, chemical formula, molar mass (M), density, pore volume (V_p), H₂ accessible surface (S), and isosteric heat of adsorption for H₂ molecule of four adm-COFs.

Figure 1 The design scheme of 1,3,5,7-tetraphenyladamantane based covalent organic frameworks (adm-COF) with ctn and bor net topology structures. For clarity, the H atoms of 1,3,5,7-tetraphenyladamantane are omitted.

Figure 2 The computed absolute (abs) and excess (exc) H₂ adsorption isotherms in four 3D adm-COF frameworks at 77 K. (a) gravimetric H₂ adsorption isotherms and (b) volumetric H₂ adsorption isotherms.

Figure 3 The computed absolute H₂ adsorption isotherms in four 3D adm-COF frameworks at 298 K. (a) gravimetric H₂ adsorption isotherms and (b) volumetric H₂ adsorption isotherms.

Figure 4 The equilibrium snapshots of four adm-COFs structure with H₂ molecules adsorbed under the pressure of 100 bar at 77 K. (a) adm-COF-1, (b) adm-COF-2, (c) adm-COF-3 and (d) adm-COF-4.

Figure 5 The schemes to synthesize the four adm-COFs based on the tetrahedral building blocks, tetra(4-dihydroxyborylphenyl)adamantane (TBPA), and the triangular building block, hexahydroxytriphenylene (HHTP). For clarity, some parts of C and D are omitted.

Table 1 The LJ potential parameters of H₂, He molecules and all the framework atoms used in the present work.

	H ₂	He	C	H	O	B
σ (Å)	2.956	2.64	3.473	2.846	3.033	3.581
ε/k_B (K)	36.7	10.9	47.856	7.649	48.156	47.806

Table 2 Unit cell parameters, chemical formula, molar mass (M), density, pore volume (V_p), H₂ accessible surface (S), and isosteric heat of adsorption (Q_{st}) for H₂ molecule of four adm-COFs.

materials	a=b=c (Å)	chemical formula	M (g/mol)	density (g/cm ³)	V_p (cm ³ /g)	S (m ² /g)	Q_{st} (kJ/mol)	
							77K	298K
adm-COF-1	33.20	C ₄₀₈ H ₃₃₆ B ₄₈ O ₄₈	6526.02	0.30	2.9095	6021.39	3.70	4.34
adm-COF-2	21.58	C ₁₀₂ H ₈₄ B ₁₂ O ₁₂	1631.51	0.27	3.2422	5967.89	3.41	4.00
adm-COF-3	49.25	C ₆₉₆ H ₄₃₂ B ₄₈ O ₉₆	10849.90	0.15	6.245	6709.18	2.38	3.02
adm-COF-4	32.13	C ₁₇₄ H ₁₀₈ B ₁₂ O ₂₄	2712.48	0.14	6.9571	6696.16	2.50	3.38

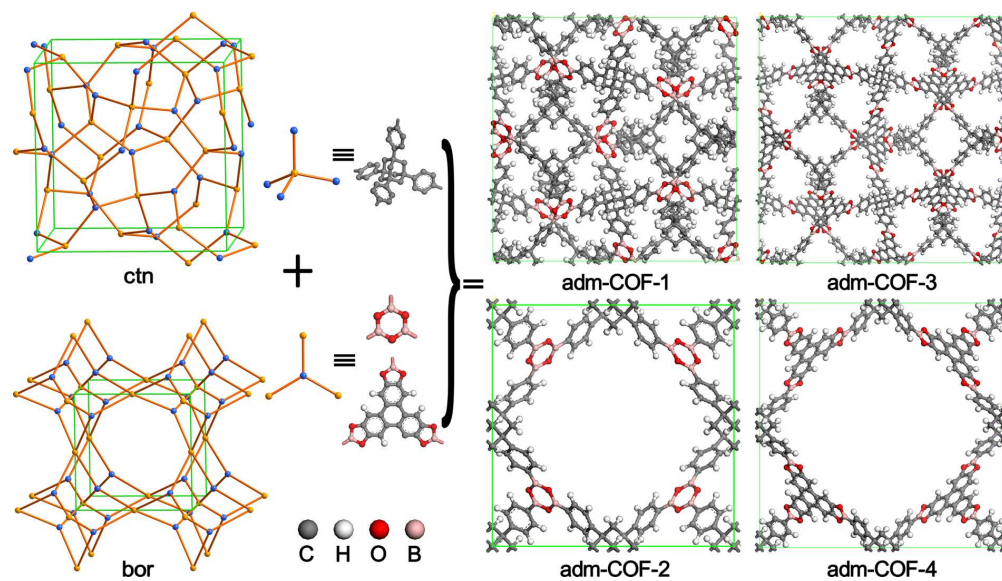


Figure 1 The design scheme of 1,3,5,7-tetraphenyladamantane based covalent organic frameworks (adm-COF) with ctn and bor net topology structures. For clarity, the H atoms of 1,3,5,7-tetraphenyladamantane are omitted.

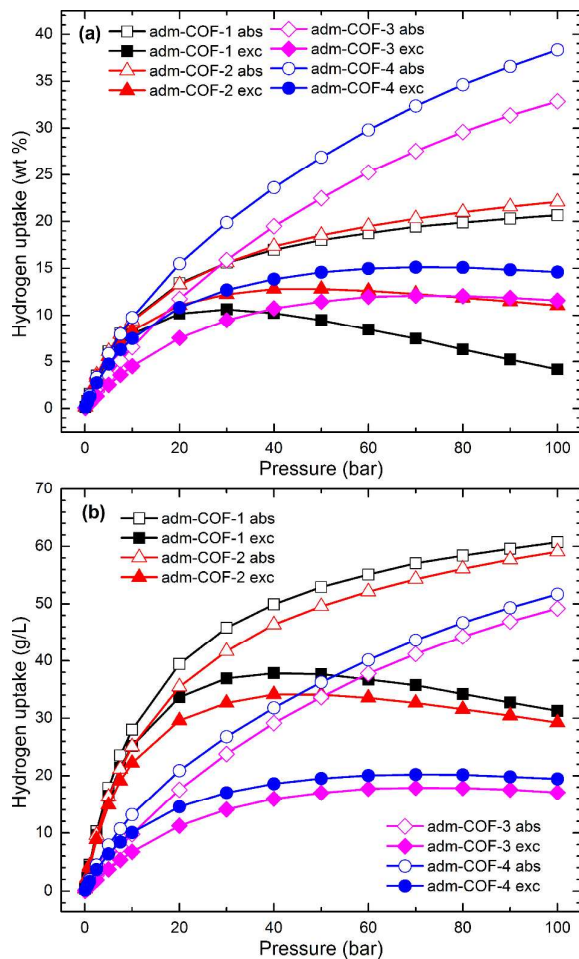


Figure 2 The computed absolute (abs) and excess (exc) H₂ adsorption isotherms in four 3D adm-COFs at 77 K. (a) gravimetric H₂ adsorption isotherms and (b) volumetric H₂ adsorption isotherms.

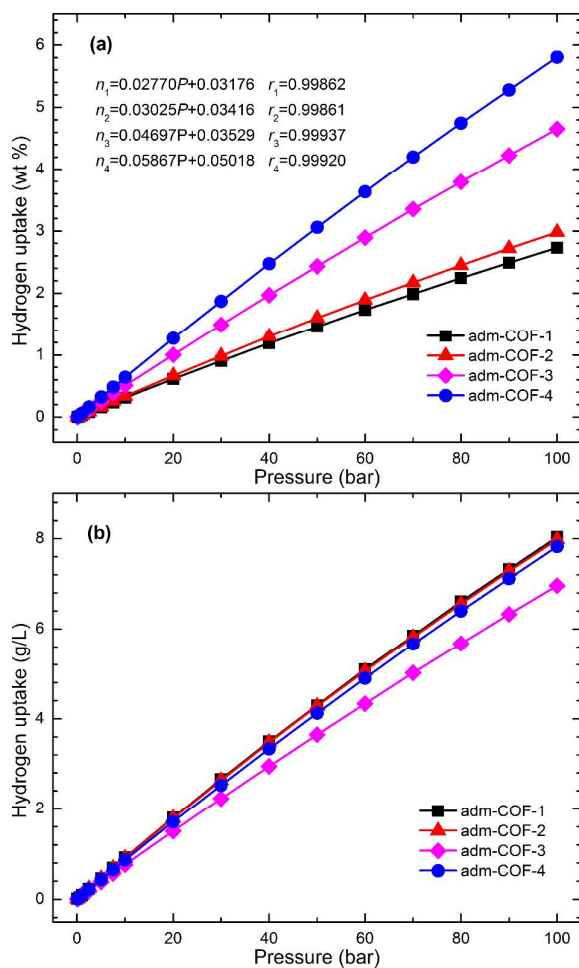


Figure 3 The computed absolute H₂ adsorption isotherms in four 3D adm-COF frameworks at 298 K. (a) gravimetric H₂ adsorption isotherms and (b) volumetric H₂ adsorption isotherms.

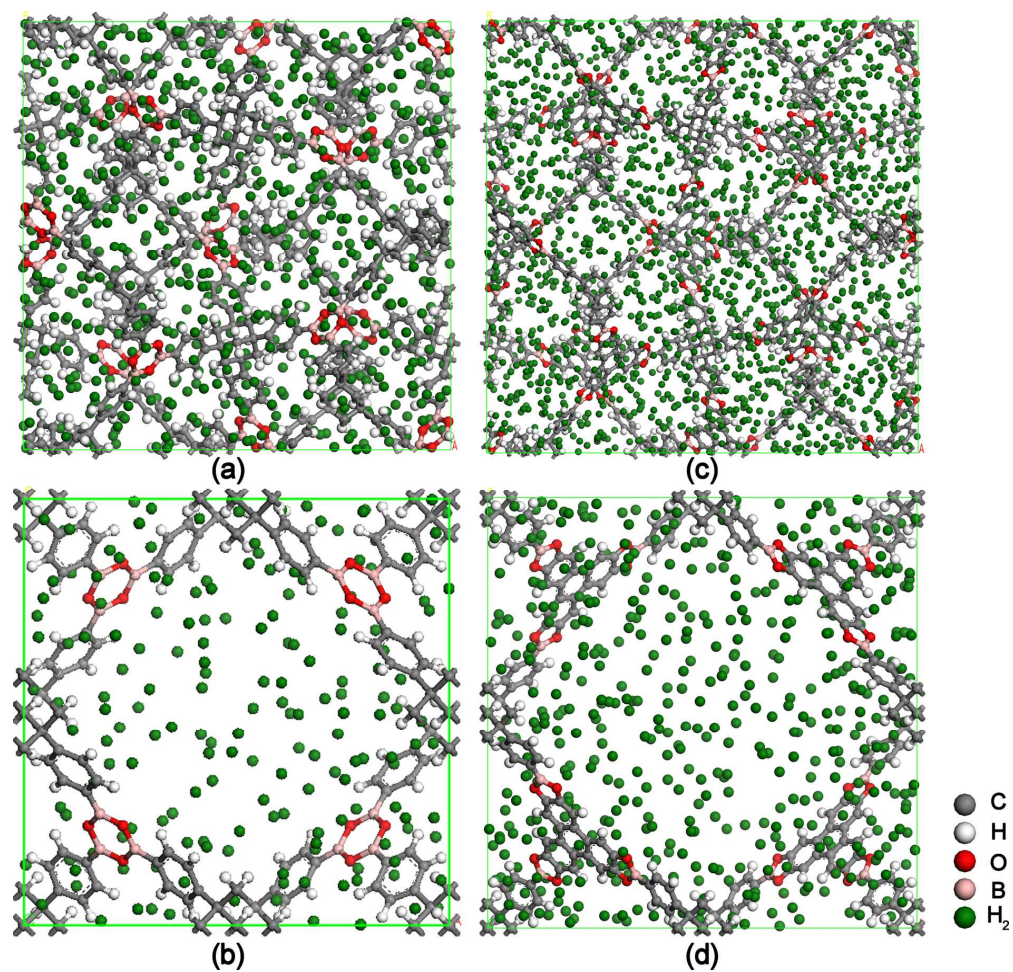


Figure 4 The equilibrium snapshots of four adm-COFs structure with H_2 molecules adsorbed under the pressure of 100 bar at 77 K. (a) adm-COF-1, (b) adm-COF-2, (c) adm-COF-3 and (d) adm-COF-4.

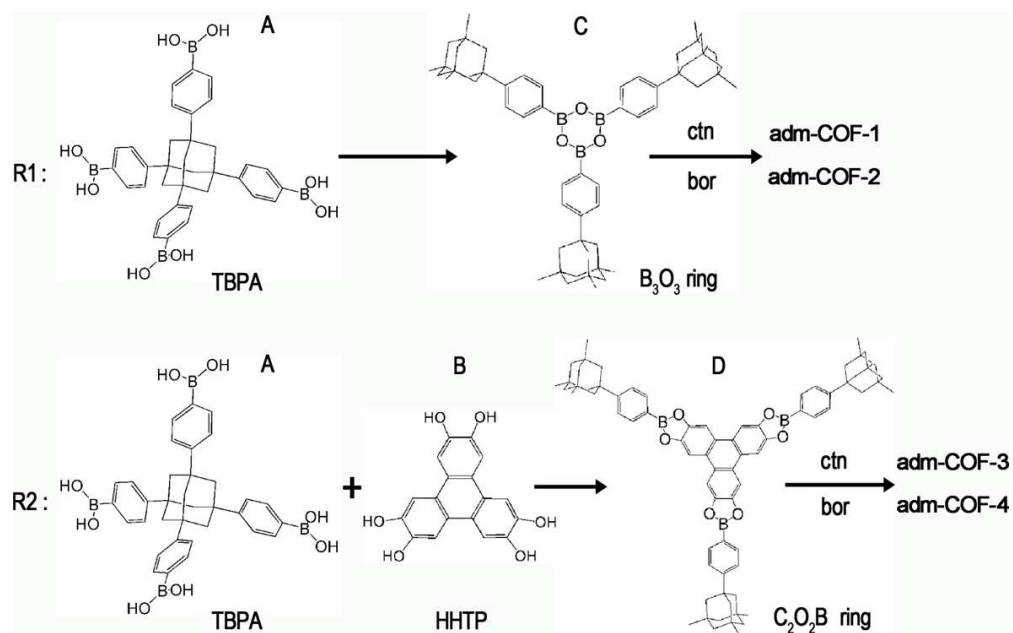


Figure 5 The schemes to synthesize the four adm-COFs based on the tetrahedral building blocks, tetra(4-dihydroxyborylphenyl)adamantane (TBPA), and the triangular building block, hexahydroxytriphenylene (HHTP). For clarity, some parts of C and D are omitted.